

function of crystal orientation about two orthogonal axes. Drawn on this figure also are circles of expected equal intensity. Clearly no significant correspondence exists. Qualitatively, the mean value of the central points (circles), in a zone of  $8 \times 10^{-3}$  radian mean angular displacement, is  $1556 \pm 13$ ; the average of the points (squares) in a zone of mean angular displacement of 0.02 radian, is  $1602 \pm 9$ ; and the average of points (triangles) in a zone of mean angular displacement of 0.035 radian is  $1541 \pm 10$ . The "expected" counts should be in the ratio 22:19.5:17.4, using the Überall calculation for a crystal temperature at absolute zero.

We find it difficult to account for this discrepancy. The effect of lattice vibration has been discussed by Überall, and on the basis of his calculations is insufficient to suppress the effect to the extent needed to fit the data. More detailed calculations on this point are in progress.<sup>4</sup> The question whether sufficient radiation dislocation could have occurred during bombardment has been examined; assuming an activation energy of 25 eV for a dislocation, only  $5 \times 10^{-6}$  of the Si atoms would have been affected. The crystals were furnished to us via Professor J. W. M. DuMond, California Institute of Technology, by Mr. W. R. Runyon of the Texas Instrument Company, Dallas. Mr. Ronald Willems, California Institute of Technology, kindly ran x-ray "rocking curves" on the crystals used: the angular half-width at half-maximum is only  $8 \times 10^{-4}$  radian; this is negligible for our considerations. Laue back-reflection pictures taken before and after our bombardments showed no observable deterioration.

We are unable to suggest an explanation for this result other than possibly the lack of validity of some of the approximations made in the calculations on the effect of lattice vibrations, or possibly of the Born approximation.

We are greatly indebted to Mr. Richard Bush, of the Stanford Department of Metallurgical Engineering, for the use of the Laue camera. We are also indebted to Professor J. W. M. DuMond for furnishing the crystals and for valuable advice. We wish to thank Dr. G. L. Pearson of Bell Telephone Laboratories, for informing us about the techniques of lapping single crystals of Si and their chemical etching.

mission, and the Air Force Office of Scientific Research.

<sup>1</sup>F. J. Dyson and H. Überall, Phys. Rev. **99**, 604 (1955).

<sup>2</sup>E. M. Purcell (private communication).

<sup>3</sup>H. Überall, Phys. Rev. **103**, 1055 (1956); CERN Report No. 58-21, September, 1958 (unpublished); and numerous private communications.

<sup>4</sup>L. I. Schiff (private communication).

### NONMESONIC/MESONIC DECAY RATIO OF HELIUM HYPERFRAGMENTS\*

Peter E. Schlein

Northwestern University,  
Evanston, Illinois

(Received October 31, 1958; revised  
manuscript received February 2, 1959)

In order to understand the decay interactions of the bound  $\Lambda^0$ ,<sup>1-6</sup> it is important that the non-mesonic/mesonic ratio ( $Q$ ) in the decay of hyperfragments be experimentally well determined. Previously reported experimental values of  $Q$  for  $\Lambda$  He ( $2.3 \pm 1.0$ ;  $1.1 \pm 0.5$ )<sup>7,8</sup> disagree with the existing calculations<sup>4,5</sup> ( $4 \leq Q \leq 10$ ). Notwithstanding the present uncertainties in the theoretical work, which have been recently discussed by Dalitz,<sup>5</sup> certain refinements in the experimental work are desirable. It is known that  $K^-$  capture stars are prolific sources of hyperfragments. Thus problems of contamination in the event samples are diminished and the increased number of events allow the results of kinematic analysis of the nonmesonic events to be studied. Track thickness ionization measurements in the Ilford fine-grain K5 and L4 emulsion allow the use of a rigid event-selection criterion.

In this emulsion experiment we have obtained 33 examples of nonmesonic decay of  $\Lambda$  He, which were produced in  $K^-$ -capture stars, had ranges  $\geq 59 \mu$ , and decayed with the formation of two visible prongs. (The  $K^-$  mesons were produced at the Bevatron; they interacted at rest.) The 33 events were selected by means of track-thickness<sup>9</sup> (profile) and gap-count measurements on the connecting tracks. The results of the profile calibration measurements made on known charge 1 and 2 tracks are shown in Fig. 1. The dotted line is seen to separate the  $Z=1$  and  $Z=2$  calibration points at all dip angles to the extent that an individual  $Z=1, 2$  track can be charge identified to  $\sim 95\%$  level-of-confidence. No  $Z=3$  calibration was necessary since the range distribution of the

\*Supported in part by the joint program of the Office of Naval Research, the U. S. Atomic Energy Com-

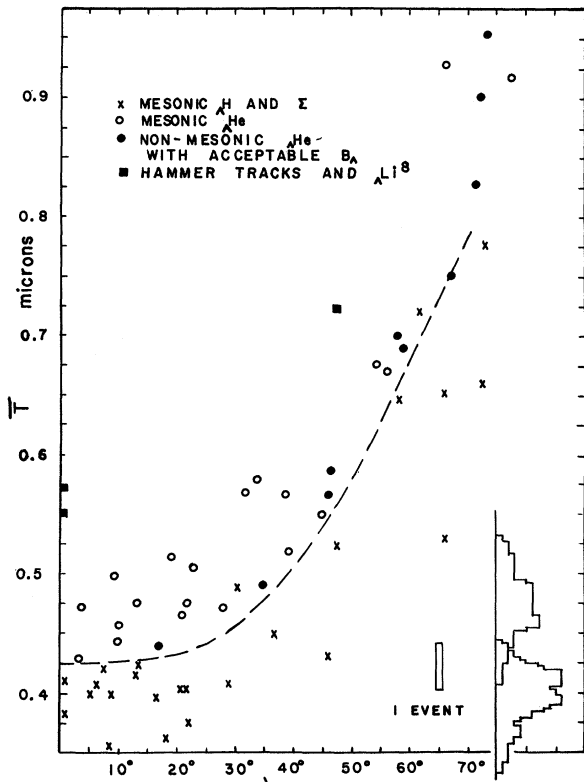


FIG. 1. Mean track thickness ( $\bar{T}$ ) vs dip angle ( $\lambda$ ) for known charge 1, 2 tracks in Ilford K5 and L4 emulsion. Thickness measurements were made at  $\sim 5000\times$  magnification with  $0.5\ \mu$  projected cell lengths from  $25\ \mu$  to  $(37/\cos\lambda)\ \mu$  residual range. The dashed line shows the optimum separation between charge 1 and 2 tracks. No dependence of  $\bar{T}$  on depth in emulsion was found. The insert shows the  $\bar{T}$  distributions for charge 1 and 2 tracks with  $\lambda < 30^\circ$ .

connecting tracks of mesonic  $\Lambda$ Li events from  $K^-$  capture stars at rest is known<sup>10</sup> to be  $< 50\ \mu$ .

In the emulsion scannings in which these hyperfragments were found, no systematic search for possible one-prong nonmesonic decays of  $\Lambda$ He was carried out. Nevertheless, one probable example of  $\Lambda$ He<sup>5</sup>  $\rightarrow$  He<sup>4</sup> +  $n$  has been found in this stack. The identification of this event is based on profile measurements of the stopping connecting track (range =  $128\ \mu$ , dip angle =  $6^\circ$ ) and of the single prong, which has the characteristic  $495\text{-}\mu$  length required for the proper energy release (dip angle of this prong is  $3^\circ$ ).

The 33 two-prong nonmesonic events are to be compared with 22 examples of  $\pi^-$ -mesonic decay of  $\Lambda$ He<sup>4,5</sup> with connecting tracks  $\geq 50\ \mu$  found in this stack. These mesonic decays have already been reported as part of the EFINS-NU (Enrico Fermi Institute of Nuclear Studies-Northwestern University) collaboration experiment<sup>10</sup> on  $\pi^-$ -

mesonic hyperfragments. It should be pointed out that on the basis of the large energy releases, none of the 33 nonmesonic events could be interpreted as  $\pi^0$ -mesonic hyperfragment decays. A scanning bias check shows the over-all efficiencies for finding the two-prong nonmesonic and  $\pi^-$ -mesonic events in the experiment to be  $\epsilon_{\text{nonmes.}} \approx \epsilon_{\text{mes.}} \approx 80\%$ . Thus the experimental ratio determined here is  $Q' = 33/22 = 1.5 \pm 0.4$ . Since the one-prong nonmesonic decays were not included in this experiment, this value must be considered as a lower limit to the total nonmesonic ratio for  $\Lambda$ He.

An attempt was made to estimate the relative frequencies of the various nonmesonic decay modes of  $\Lambda$ He<sup>4,5</sup> in our sample. With the use of an IBM-650 hyperfragment analysis program,<sup>11</sup> the two-prong nonmesonic events considered in this experiment were subjected to the following analysis.

For each event, the residual momentum of the two charged particles (all permutations of  $Z = 1$ ,  $A = 1, 2, 3$  prong identifications were assumed) was attributed to one neutron and the binding energy of the  $\Lambda^0$  ( $B_\Lambda$ ) was then calculated for that assumption. For each event the resultant  $B_\Lambda$  closest to the known mean  $B_\Lambda$  from the study of mesonic  $\Lambda$ He decays<sup>10</sup> (2.3 Mev) was selected. The dotted curve in Fig. 2 is the expected  $B_\Lambda$  distribution based on the mean  $B_\Lambda$  for  $\Lambda$ He<sup>4,5</sup> and a standard deviation of 3.2 Mev resulting from the experimental range straggling and angle-measurement uncertainties in the nonmesonic events. 23 events have  $B_\Lambda$ 's which fall within the 98% area limits of the Gaussian. Those events are considered to be kinematically identified, and their  $B_\Lambda$ 's are plotted in Fig. 2. All the possible nonmesonic decay modes of  $\Lambda$ He<sup>4,5</sup> are shown in Table I with the number of identified events of each mode in our sample. From the  $B_\Lambda$  distribution of the 10 "background" events (i.e., those with  $B_\Lambda < -5.6$  or  $B_\Lambda > 10.4$  Mev), it can be estimated that 3 of the 23 identified events may be misidentified. The 10 "background" events are assumed to have 2 or 3 neutrons emitted and thus are examples of modes  $c5$ ,  $c5'$ , or  $c4$ .

In accordance with the recent work of Baldo-Ceolin *et al.*<sup>12</sup> and Ferrari and Fonda,<sup>6</sup> modes  $a5$  and  $a4$  in Table I are referred to as proton-stimulated decays and modes  $e5'$  and  $c4$  as neutron-stimulated decays [i.e.,  $\Lambda^0 + (p \text{ or } n) \rightarrow n + (p \text{ or } n)$ ]. The prong momentum distributions in the decay modes  $a5$  and  $a4$  (see Fig. 3) are of interest, for we see that the proton and neutron

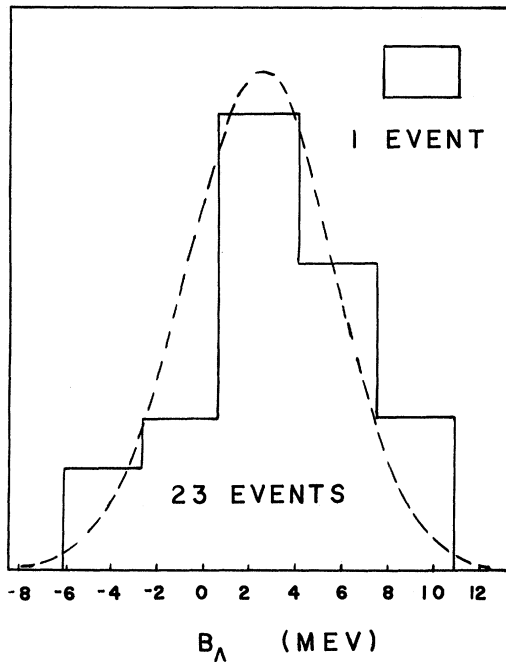


FIG. 2.  $B_{\Lambda}$  distribution for those  $\Lambda$ He events which furnish acceptable binding energies (see text). The dashed curve is the expected distribution based on the known  $B_{\Lambda}$  for  $\Lambda$ He<sup>4,5</sup> and a 3.2-MeV standard deviation caused by range straggling and angle-measurement uncertainties in the nonmesonic events.

momentum distributions are similar. This is consistent both with our identification of these events and with the single nucleon stimulation picture.

Those events which decay via mode  $b5$  do not represent simple cases of stimulated decay of the  $\Lambda^0$ . They can be interpreted either in terms of a two-nucleon stimulation process or of the

Table I. Nonmesonic decay modes of  $\Lambda$ He<sup>4,5</sup>. The numbers in parentheses refer to events for which no single acceptable  $B_{\Lambda}$  results from the kinematic analysis. Except for the one indicated event, modes  $e4$ ,  $e5$ ,  $e5'$  were excluded from consideration in this experiment.

	$\Lambda$ He <sup>5</sup>	Number of events	$\Lambda$ He <sup>4</sup>
(a5)	$H^3 + H^1 + n$	8 (2)	$H^2 + H^1 + n$ (a4)
(b5)	$H^2 + H^2 + n$	5	
(c5)	$H^2 + H^1 + 2n$	(10)	$H^1 + H^1 + 2n$ (c4)
(c5')	$H^1 + H^1 + 3n$		
(d5)	$H^3 + H^2$	0	$H^3 + H^1$ (d4)
		0	$H^2 + H^2$ (d4')
(e5)	$He^4 + n$	1	$He^3 + n$ (e4)
(e5')	$He^3 + n + n$	...	

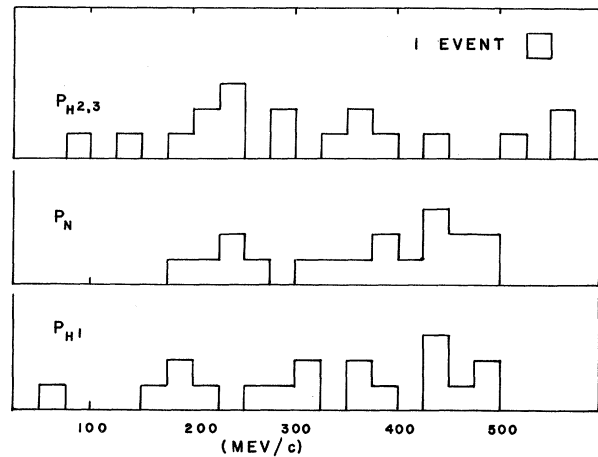


FIG. 3. The particle momentum distributions in those events which were kinematically identified as  $\Lambda$ He<sup>4,5</sup>  $\rightarrow$   $H^2, 3 + H^1 + n$ .

existence of the intermediate states  $H^3 + H^1 + n$  or  $He^3 + 2n$  with subsequent final-state interaction<sup>13</sup> producing  $2H^2 + n$ .

The inclusion of the one-prong nonmesonic decays of  $\Lambda$ He<sup>4,5</sup> in an experimental determination of the total nonmesonic decay rate is a necessary consideration in the planning of future hyperfragment experiments. In particular, mode  $e5'$  must be included in an experimentally determined neutron/proton stimulation ratio. The identification of this neutron-stimulated decay mode of  $\Lambda$ He<sup>5</sup> presents a difficult problem, however, for the  $He^3$  prong can have a wide range of values. If the recoil ( $He^3$ ) momentum distribution in these decays is similar to the recoil ( $H^2, 3$ ) momentum distribution in the proton-stimulated decays of  $\Lambda$ He<sup>4,5</sup>, then the  $P_{H^{2,3}}$  distribution in Fig. 3 tells us that  $\sim 80\%$  of the  $He^3$  prongs in mode  $e5'$  will have ranges  $\geq 70 \mu$ . The appearances of modes  $e4$  and  $e5$  are self-evident because of the characteristic prong lengths and should provide no particular difficulties. The one example of  $e5$  reported here and a possible example of  $e4$  reported by Silverstein<sup>8</sup> point out the existence of these modes.

I am grateful to Professor J. Roberts, Professor L. Brown, and Professor M. Peshkin for consultation and continued encouragement, and to Dr. S. Limentani and Phillip Steinberg for collaboration on the mesonic decay work and in setting up the profile-measuring microscope.

\*This research was supported by the National Science Foundation and the U. S. Atomic Energy Commission

through an Argonne National Laboratory subcontract.

<sup>1</sup>W. Cheston and H. Primakoff, Phys. Rev. 92, 1537 (1953).

<sup>2</sup>H. Primakoff, Nuovo cimento 3, 1394 (1956).

<sup>3</sup>T. K. Fowler, Phys. Rev. 102, 844 (1956).

<sup>4</sup>M. Ruderman and R. Karplus, Phys. Rev. 102, 247 (1956).

<sup>5</sup>R. H. Dalitz, Phys. Rev. 112, 605 (1958); see also R. H. Dalitz, Revs. Modern Phys. (to be published).

<sup>6</sup>F. Ferrari and L. Fonda, Nuovo cimento 7, 320 (1958).

<sup>7</sup>Schneps, Fry, and Swami, Phys. Rev. 106, 1062 (1957).

<sup>8</sup>Elliot Silverstein, thesis, University of Chicago, 1958 [Suppl. Nuovo cimento (to be published)].

<sup>9</sup>I am grateful to Professor U. Camerini, Professor W. F. Fry, and Dr. S. Limentani for several invaluable discussions on the experimental difficulties in the use of track thickness measurements for charge determination. See also Nakagawa, Tamai, Huzita, and Okudaira, J. Phys. Soc. Japan 11, 191 (1956).

<sup>10</sup>Ammar, Levi-Setti, Limentani, Schlein, Slater, and Steinberg, Proceedings of the 1958 Annual International Conference on High-Energy Physics at CERN, edited by B. Ferretti (CERN, Geneva, 1958).

<sup>11</sup>Fred Inman, thesis, University of California Radiation Laboratory Report UCRL-3815, 1957 (unpublished).

<sup>12</sup>Baldo-Ceolin, Dilworth, Fry, Greening, Huzita, Limentani, and Sichirollo, Nuovo cimento 7, 328 (1958).

<sup>13</sup>The existence of an interaction between the heavy final state particles in the mesonic decay of  $\Lambda$ He<sup>5</sup> has been demonstrated by the results of the EFINS-NU collaboration experiment on  $\pi^-$ -mesonic decays<sup>10</sup> and the theoretical calculations by Cottingham and Byers (1958) and Brown, Peshkin, and Snow (1958) (private communications).

#### NATURE OF THE VECTOR INTERACTION IN $\mu^-$ -ABSORPTION\*

Steven Weinberg

Columbia University,  
New York, New York

(Received February 5, 1959)

Feynman and Gell-Mann have suggested<sup>1</sup> that the strangeness-conserving vector lepton interaction current  $J_\lambda^{(V)}$  is conserved, and equal (up to a constant  $C_V/e$ , and an isospin rotation) to the isovector part of the electromagnetic current. The  $\beta$ -decay experiments that have been suggested that might test this idea are either very difficult because the "weak-magnetism" effects are very small and easily masked by Cou-

lomb and other effects,<sup>2,3</sup> or do not unambiguously distinguish between the new theory and any reasonable model of nuclear decay.<sup>4</sup> Therefore, one is naturally led to consider, instead of  $\beta$ -decay, the very high momentum-transfer process of  $\mu^-$  absorption.<sup>5</sup> We wish to suggest that a comparison of the rate of any  $0 \rightarrow 0$   $\mu^-$  capture, with the cross section for the corresponding inelastic electron scattering process, may serve as a definitive test of the Feynman-Gell-Mann proposal.

In general, the transition probability for a process  $\mu^- + A \rightarrow \nu + B$  will depend on matrix elements of the vector and the axial-vector currents. In order to test a theory of the vector interaction it is necessary to consider the case where  $A, B$  have zero spin and equal parity so that the axial current cannot contribute. Since  $A$  must be fairly stable it must necessarily be the ground state of an even-even nucleus; then  $B$  is some state of an odd-odd nucleus. The total rate for the particular transition  $A \rightarrow B$  is given by

$$\omega = \frac{2Z_A^3 \alpha^3 m_\mu^5 m_A^4 P_\nu^4}{(2\pi)^6 (m_\mu + m_A)^4 (q^2)^2} |F(q^2) C_V \sqrt{2}|^2, \quad (1)$$

where the function  $F(q^2)$  is defined, for conserved currents, by

$$\langle B | J_\lambda^{(V)} | A \rangle = (2\pi)^{-3} (4m_A E_B)^{-1/2} F(q^2) C_V \sqrt{2} \\ \times \{ (P_B + P_A)_\lambda - [(m_A^2 - m_B^2)/q^2] (P_B - P_A)_\lambda \}, \quad (2)$$

and  $q^2$  is the invariant momentum transfer,

$$q^2 \equiv (P_A - P_B)^2 = m_\mu^2 - \frac{m_\mu (m_\mu^2 + m_B^2 - m_A^2)}{m_\mu + m_A} \sim (100 \text{ Mev}/c)^2. \quad (3)$$

Now suppose that  $A$  is an isospin singlet, that  $B$  has  $T=1$ ,  $T_3=-1$ , and that  $A^*$  is the excited state of  $A$  belonging to the same triplet as  $B$ . The inelastic electron scattering process,  $e + A \rightarrow e + A^*$ , has a matrix element given by the Feynman-Gell-Mann theory as

$$\langle A^* | J_\lambda^{(el)} | A \rangle = (2\pi)^{-3} (4m_A E_{A^*})^{-1/2} F(q^2) e \\ \times \{ (P_{A^*} + P_A)_\lambda - [(m_A^2 - m_{A^*}^2)/q^2] (P_{A^*} - P_A)_\lambda \}, \quad (4)$$

where  $J_\lambda^{(el)}$  is the electric current,  $q^2 = (P_A - P_{A^*})^2$ , and  $F(q^2)$  is the same as in (2). The differential cross section is then given by

$$\left( \frac{d\sigma}{d\Omega} \right)_{\text{lab}} = \frac{\alpha^2 \cos^2(\theta/2) |F(q^2)|^2}{4E_e [E_e + (m_A^2 - m_{A^*}^2)/2m_A] \sin^4(\theta/2) [1 + (2E_e/m_A) \sin^2(\theta/2)]}, \quad (5)$$